

Nature of the unusual transient AT 2018cow from H_I observations of its host galaxy[★]

Michał J. Michałowski¹, P. Kamphuis², J. Hjorth³, D. A. Kann⁴, A. de Ugarte Postigo^{4,3}, L. Galbany⁵, J. P. U. Fynbo⁶, A. Ghosh⁷, L. K. Hunt⁸, H. Kuncarayakti^{9,10}, E. Le Floch¹¹, A. Leśniewska¹, K. Misra^{7,12}, A. Nicuesa Guelbenzu¹³, E. Palazzi¹⁴, J. Rasmussen^{3,15}, L. Resmi¹⁶, A. Rossi¹⁴, S. Savaglio¹⁷, P. Schady¹⁸, S. Schulze¹⁹, C. C. Thöne⁴, D. Watson⁶, G. I. G. Józsa^{20,21,22}, P. Serra²³, and O. M. Smirnov^{21,20}

(Affiliations can be found after the references)

Received 26 February 2019 / Accepted 7 June 2019

ABSTRACT

Context. Unusual stellar explosions represent an opportunity to learn about both stellar and galaxy evolution. Mapping the atomic gas in host galaxies of such transients can lead to an understanding of the conditions that trigger them.

Aims. We provide resolved atomic gas observations of the host galaxy, CGCG137-068, of the unusual and poorly understood transient AT 2018cow, which we obtained in searching for clues to understand its nature. We test whether it is consistent with a recent inflow of atomic gas from the intergalactic medium, as suggested for host galaxies of gamma-ray bursts (GRBs) and some supernovae (SNe).

Methods. We observed the H_I hyperfine structure line of the AT 2018cow host with the Giant Metrewave Radio Telescope.

Results. There is no unusual atomic gas concentration near the position of AT 2018cow. The gas distribution is much more regular than the distributions of GRB/SN hosts. The AT 2018cow host has an atomic gas mass lower by 0.24 dex than predicted from its star formation rate (SFR) and is at the lower edge of the galaxy main sequence. In the continuum we detected the emission of AT 2018cow and of a star-forming region in the north-eastern part of the bar (away from AT 2018cow). This region hosts a third of the galaxy's SFR.

Conclusions. The absence of atomic gas concentration close to AT 2018cow, along with a normal SFR and regular H_I velocity field, sets CGCG137-068 apart from GRB/SN hosts studied in H_I. The environment of AT 2018cow therefore suggests that its progenitor may not have been a massive star. Our findings are consistent with an origin of the transient that does not require a connection between its progenitor and gas concentration or inflow: an exploding low-mass star, a tidal disruption event, a merger of white dwarfs, or a merger between a neutron star and a giant star. We interpret the recently reported atomic gas ring in CGCG 137-068 as a result of internal processes connected with gravitational resonances caused by the bar.

Key words. dust, extinction – galaxies: individual: CGCG137-068 – galaxies: ISM – galaxies: star formation – radio lines: galaxies – supernovae: individual: AT 2018cow

1. Introduction

Unusual, luminous, and rare stellar explosions provide an opportunity to learn about stellar evolution and also about galaxy evolution in a broader context. An example of the latter approach is the possibility of selecting galaxies that experience a recent inflow of gas from the intergalactic medium (IGM) using host galaxies of long gamma-ray bursts (GRBs) and some types of supernovae (SN). Atomic gas concentrations away from the galaxy centres towards GRB/SN positions suggest an external origin of the gas (Michałowski et al. 2015, 2016, 2018a), and a potential deficiency in molecular gas (Hatsukade et al. 2014; Stanway et al. 2015; Michałowski et al. 2016, 2018b). Studying gas inflows in such a direct way is important because they are required to fuel star formation in all galaxies, as implied from observations (Sancisi et al. 2008; Sánchez et al. 2014; Spring & Michałowski 2017; Elmegreen et al. 2018; Combes 2018) and simulations (Schaye et al. 2010; van de Voort et al. 2012; Narayanan et al. 2015). Recently, Thöne et al. (2019) also suggested that in GRB hosts gas outflows are very common.

Observations of atomic gas in host galaxies of unusual and/or unclassified transients can therefore bring us closer to understanding the nature of these events. Similar atomic gas properties around the position of a transient to those of GRBs would suggest that the explosion mechanism is similar, that is, an explosion of a massive star.

With this in mind, we report an analysis of gas properties in the host galaxy of the unusual and poorly understood transient AT 2018cow¹. The transient was discovered on 16 June 2018 by the Asteroid Terrestrial-impact Last Alert System (ATLAS; Tonry et al. 2018) surveying the entire visible sky every two nights (Smartt et al. 2018; Prentice et al. 2018). It was classified as a broad-lined type Ic (Izzo et al. 2018; Xu et al. 2018), type Ib (Benetti et al. 2018), or interacting type Ibn (Fox & Smith 2019) supernova and given the designation SN 2018cow. However, it is unclear whether this really was a supernova (see below). It has been detected at (sub)millimetre (de Ugarte Postigo et al. 2018; Smith et al. 2018; Ho et al. 2019) and radio (Dobie et al. 2018; Bright et al. 2018; Nayana & Chandra 2018; Margutti et al. 2019) wavelengths, including very long-baseline interferometry (VLBI), from which the most precise position has been derived: RA (J2000) = 16:16:00.2243, Dec (J2000) = +22:16:04.893 with

[★] The HI data cube and moment maps are only available at the CDS via anonymous ftp to cdsarc.u-strasbg.fr (130.79.128.5) or via <http://cdsarc.u-strasbg.fr/viz-bin/qcat?J/A+A/627/A106>

¹ It was initially designated ATLAS 18qqn by the ATLAS discovery team.

a ~ 1 mas uncertainty (An 2018; Bietenholz et al. 2018; Horesh et al. 2018). AT2018cow had several unusual characteristics: high peak luminosity, blue colour and high temperature even a month after the explosion, very fast initial flux rise (Prentice et al. 2018; Perley et al. 2019), high decline rate, no spectral features up to four days after the explosion, very broad short-lived absorption and emission spectral features (Perley et al. 2019), variability of the X-ray light curve (Rivera Sandoval et al. 2018), a month-long plateau at millimetre wavelengths (see Michałowski et al. 2018c for another example), and high radio flux (Ho et al. 2019).

It has been shown that it could not have been powered by radioactive decay (Prentice et al. 2018; Margutti et al. 2019; Perley et al. 2019). Several models have been proposed to explain the observed properties: a stellar collapse leading to the formation of a magnetar (Prentice et al. 2018; Margutti et al. 2019), a luminous blue variable exploding in a non-uniform circum-stellar medium (Rivera Sandoval et al. 2018), a SN from a low-mass hydrogen-rich star, a failed SN from a blue supergiant (Margutti et al. 2019), a tidal disruption event (TDE; Liu et al. 2018; Kuin et al. 2019; Perley et al. 2019), a jet driven by an accreting neutron star colliding with a giant star (Soker et al. 2019), or a merger of white dwarfs (Lytikov & Toonen 2018). However, the constraints on the nature of this explosion set by the host galaxy properties have not been explored thoroughly.

AT2018cow exploded within a spiral galaxy of type Sc (Willett et al. 2013), CGCG 137-068, at a redshift of $z = 0.014$ (Perley et al. 2019). It has an inclination from the line of sight of 24.4° (Makarov et al. 2014)². It has a bar and weak spiral arms (Perley et al. 2019). Its stellar mass and star formation rate (SFR) are $1.42^{+0.17}_{-0.29} \times 10^9 M_\odot$ and $0.22^{+0.03}_{-0.04} M_\odot \text{ yr}^{-1}$, respectively (Perley et al. 2019). The galaxy was claimed to be asymmetric with more near-IR emission in the south-west, that is, in the part of the galaxy where AT2018cow exploded (Kuin et al. 2019), ~ 1.7 kpc from the galaxy centre (Kuin et al. 2019; Perley et al. 2019).

The objectives of this paper are i) to provide a resolved measurement of the atomic gas properties of the host galaxy of AT2018cow in order to learn about its nature, and ii) to test whether these properties are consistent with a recent inflow of atomic gas from the intergalactic medium.

We use a cosmological model with $H_0 = 70 \text{ km s}^{-1} \text{ Mpc}^{-1}$, $\Omega_\Lambda = 0.7$, and $\Omega_m = 0.3$, implying that AT2018cow, at $z = 0.014$, is at a luminosity distance of 60.6 Mpc and $1''$ corresponds to 286 pc at its redshift. We also assume the Chabrier (2003) initial mass function (IMF).

2. Data

On 8 and 9 February 2019, the field of AT2018cow was observed for 14 h with the Giant Metrewave Radio Telescope (GMRT)³. For calibration of the flux and the bandpass, 3C286 was observed for 15 min at the start and end of the run. For the phase calibration 1609+266 was observed every 40 min. The correlator was set up with 33 MHz bandwidth and 512 channels centred around 1400 MHz.

After the submission of this paper, additional GMRT data were reported by Roychowdhury et al. (2019). Hence, for the HI analysis we also included these archival data⁴. As part of that program, 7 h of data were obtained on 27 August 2018. The

channel width was half as wide as for our observations. The same calibrators were observed.

The data were reduced with a range of data-reduction packages. We downloaded the FITS files with the raw data from the GMRT archive. These FITS files were then loaded into the Common Astronomy Software Applications (CASA) package (McMullin et al. 2007) with the `IMPORTGMRT` task without applying the online flags. The data were further reduced with the `MEERKATHI`⁵ pipeline, which is being developed for HI data reduction of MeerKAT data. The pipeline is set up in a modular fashion using the platform-independent radio interferometry scripting framework `STIMELA`⁶. In practice this means that the calibrator data are initially flagged with `AOFLAGGER` (Offringa 2010) and calibrated and transferred to the target with CASA. For the data in this paper, the phase calibrator was used as a bandpass calibrator, as the GMRT bandpass clearly fluctuated over the time of the observations. As the phase calibrator was bright (4.8 Jy), this leads to an improved bandpass calibration over the course of the observations.

After the initial calibration, the target was split out of the measurement set, further flagged with `AOFLAGGER`, imaged with `WSCLEAN` (Offringa et al. 2014) in Stokes I, then the sources in the field were extracted and modelled with `pyBDSF`⁷, after which this model was used in `Cubical`⁸ (Kenyon et al. 2018) for the self-calibration. This step was repeated until a phase-only self-calibration no longer improved the extracted models.

After the calibration, the three separate days were mapped onto the same channel grid with the CASA task `MSTRANSFORM` and the modelled continuum was subtracted from the data. Any residual continuum was subtracted with `UVLIN`. At this stage the data were also Doppler-corrected and projected onto a barycentric velocity frame.

The visibilities were weighted according to a Briggs weighting scheme with `Robust = 0.0` and `uvtapers` of 4, 6, 8 and 20 k λ were applied to attain cubes with varying spatial resolution. The cubes were inverted and cleaned with the CASA task `TCLEAN`. The cleaning was performed in an iterative process where we first cleaned the full cube to a 10σ threshold, then created a mask with `SoFiA` (Serra et al. 2015), and then cleaned within this mask to 0.5σ . This last step was done outside the pipeline as currently it cannot deal with the frequency increments of opposite sign in the different datasets.

The final cubes have a resolution of $FWHM = 28''9 \times 26''2$, $19''2 \times 18''1$, $13''12 \times 12''9$, and $5''5 \times 4''6$ and a channel width of 65.1 kHz. The frequency axis was converted into a velocity axis using the relativistic definition, which results in a channel width of 13.9 km s^{-1} with an error of $\sim 0.01 \text{ km s}^{-1}$ on the outermost channels of the cube.

For our data from February 2019 (excluding those from August 2018 because of the variability of AT2018cow), we also imaged together all channels of the entire 33 MHz bandwidth (before continuum subtraction) to produce a continuum image at an observed frequency of 1.397667 GHz. The beam size is $2.0'' \times 1.8''$ and the noise is $17.5 \mu\text{Jy beam}^{-1}$. The HI line spans ~ 0.6 MHz, so it should not affect this continuum image based on the 33 MHz bandwidth. When we exclude the channels with the line emission, we obtain an almost identical map.

In order to correct the astrometry, we identified 16 sources in the Faint Images of the Radio Sky at Twenty-Centimeters

² <http://leda.univ-lyon1.fr/ledacat.cgi?CGCG%20137-068>

³ Project no. 35_021, PI: M. Michałowski.

⁴ Project no. DDTC022, PI: M. Arabsalmani.

⁵ <https://github.com/ska-sa/meerkathi-public>, a private repository for the time of development.

⁶ <https://github.com/SpheMakh/Stimela/wiki>

⁷ <https://github.com/lofar-astron/PyBDSF>

⁸ <https://github.com/ratt-ru/CubiCal/>

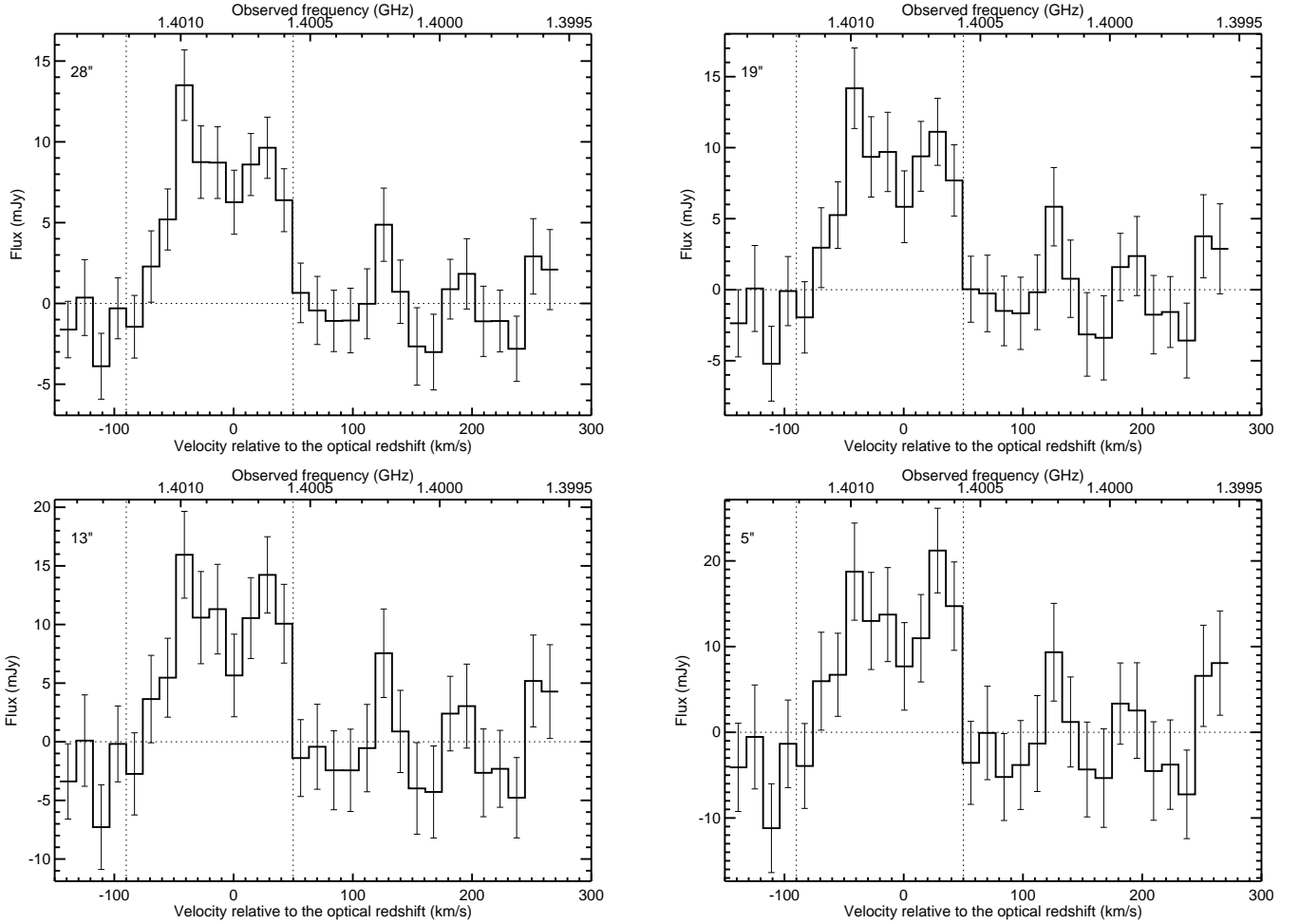


Fig. 1. H I spectra of CGCG 137-068 extracted over the entire galaxy within an aperture of $45''$ radius (solid histogram) derived from the data cubes with resolutions as marked on the panels. The dotted lines denote the velocity range over which the total H I was estimated.

(FIRST) survey (Becker et al. 1995; White et al. 1997) that are point-like in our continuum map. On average, these sources were found to be shifted on our map with respect to the FIRST position by $(+1.30 \pm 0.14)''$ in right ascension and $(+0.51 \pm 0.14)''$ in declination. We shifted our continuum and H I maps by this offset. This has very little effect on H I maps, as their beam sizes are much larger. This offset also implies that the positional uncertainty in our continuum map is $0.14''$ in both directions.

3. Results

The H I fluxes at each frequency element were determined by aperture photometry with an aperture radius of $45''$. The spectra are shown in Fig. 1. The H I emission maps derived from the collapsed cubes within the dotted lines in Fig. 1 are shown in Fig. 2. This range was selected to encompass the full velocity width of the line. It was also used to obtain integrated H I emission (F_{int} in Jy km s^{-1}) directly from the spectra. The line luminosity (L'_{HI} in $\text{K km s}^{-1} \text{pc}^2$) was calculated using Eq. (3) in Solomon et al. (1997) and transformed into M_{HI} using Eq. (2) in Devereux & Young (1990). The H I zeroth- and first-moment maps (integrated emission and velocity field) are also shown in Fig. 2.

We detected and resolved the H I emission of the host of AT 2018cow. The atomic gas disc is larger than the stellar disc with a centre (moment 0 “centre of mass”) offset from the optical centre by $\sim 1\text{--}2''$ ($\sim 0.3\text{--}0.6$ kpc in projection), and $\sim 5\text{--}6''$ or

$\sim 1.4\text{--}1.7$ kpc from the position of AT 2018cow. When the formula of Ivison et al. (2007)⁹ is used, the positional uncertainty is $\sim 0.5\text{--}1.5''$, so the offset of the H I emission centre to the galaxy centre is at most 2σ , but to the position of AT 2018cow, it is significant at $\sim 5\sigma$.

The H I maps (Fig. 2) do not show strong evidence of recent gas inflows. The gas distribution is much more regular than those of the hosts of GRB 980425 (Arabsalmani et al. 2015), GRB 060505 (Michałowski et al. 2015), and SN 2009bb (Michałowski et al. 2018a), which exhibit high gas concentrations close to the GRB/SN positions, away from the galaxy centres.

On the two zeroth-moment maps with the highest resolutions we see the ring-like structure reported by Roychowdhury et al. (2019). In Sect. 4 we provide evidence that this structure is of internal origin.

On the outskirts of CGCG 137-068 are gas plumes in both the zeroth-moment and the collapsed maps (Fig. 2), but they have a low signal-to-noise ratio, so they cannot confidently be interpreted as real structures. Moreover, they might be spiral structures.

Moreover, from one resolution to another, the centre of mass of the zeroth-moment maps moves only by $\sim 1''$ ($\sim 3''$ for the $28''$ map with the lowest positional uncertainty). This suggests that the distribution is symmetric. The velocity fields (bottom row of

⁹ $r = 0.6 \times FWHM_{\text{beam}}/(S/N)$, where $FWHM_{\text{beam}}$ is the FWHM of the beam.

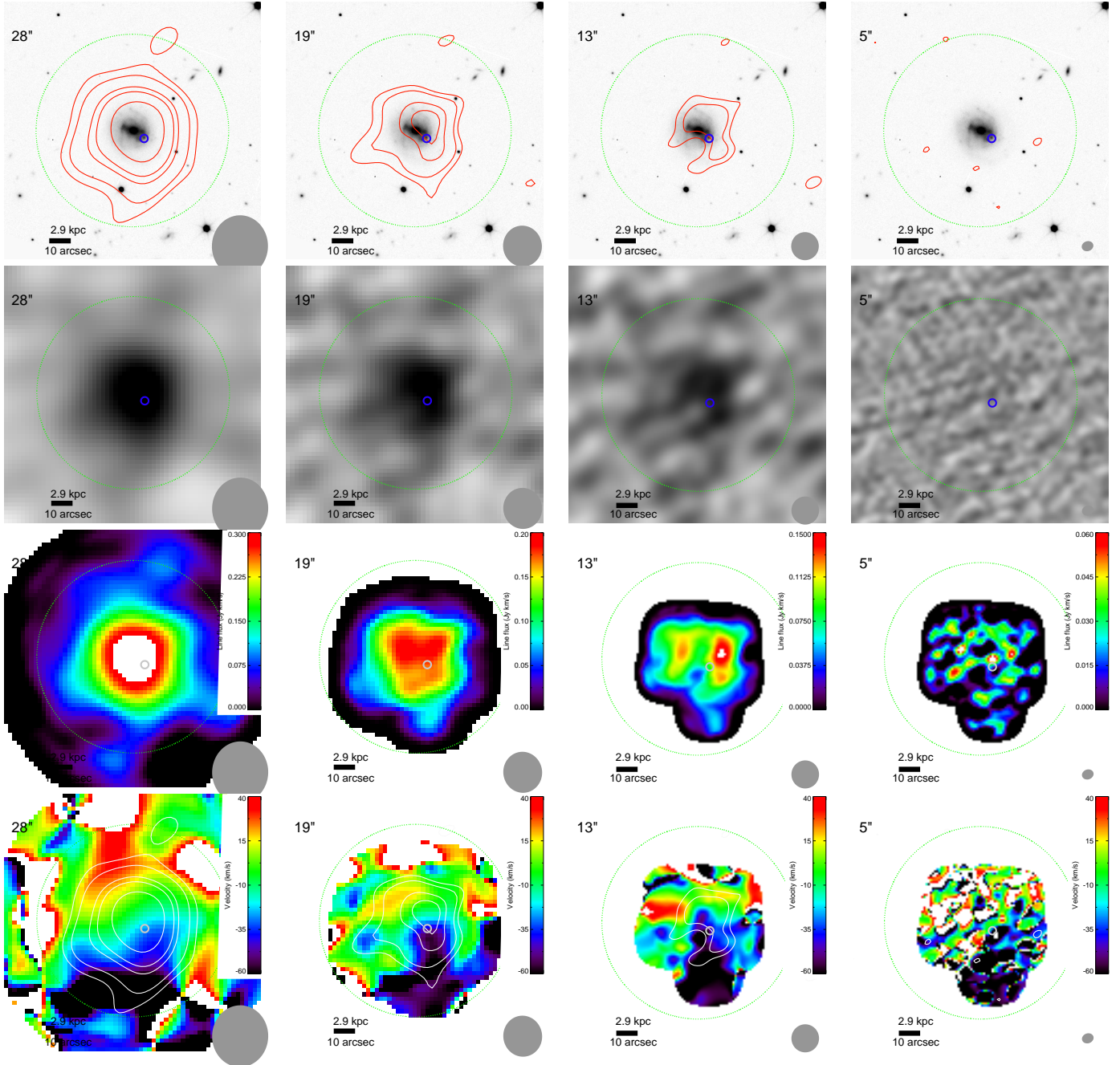


Fig. 2. *Top:* HI contours (red; collapsed HI cube) of CGCG 137-068 overlaid on the Gran Telescopio Canarias optical i' -band image (Kann et al., in prep.). The contours are 3, 4, 6, 7, and 9σ , where $\sigma = 0.031, 0.029, 0.027,$ and $0.019 \text{ Jy beam}^{-1} \text{ km s}^{-1}$ for the data at the resolution of $28'', 19'', 13'',$ and $5''$, respectively (corresponding to a neutral hydrogen column density of $\sim 0.5, 0.9, 1.8,$ and $8.4 \times 10^{20} \text{ cm}^{-2}$, respectively). *Second row:* HI data cube collapsed within the dotted lines given in Fig. 1. *Third row:* zeroth-moment map (integrated emission) of the HI line. *Bottom:* first-moment map (velocity field) of the HI line with the same contours as in the top panel. The velocities are relative to the systemic velocity of 4197 km s^{-1} derived from the optical spectrum (Perley et al. 2019). Columns are for the resolution as marked in the panels. The VLBI position of AT 2018cow is indicated by the blue or grey circles. The green dotted circle has a radius of $45''$ and corresponds to the aperture within which the total HI emission was measured. The beam size of the HI data is shown as the grey ellipses. The images are $120'' \times 120''$, and the scale is indicated by the ruler. North is up and east is to the left.

Fig. 2) and the double-horn profiles of the HI spectra (Fig. 1) are consistent with a rotating disc.

The SFR- M_{HI} relation (Eq. (1) in Michałowski et al. 2015) predicts $\log(M_{\text{HI}}/M_{\odot}) = 9.14^{+0.04}_{-0.07}$ for $\text{SFR} = 0.22 M_{\odot} \text{ yr}^{-1}$ of CGCG 137-068 (the errors include both the uncertainty in the SFR and in the parameters of the relation). This is 0.24 dex, that is, $\sim 3\sigma$, higher than the measured value (Table 1), which

is within the scatter of this relation (0.38 dex at 1σ). Hence CGCG 137-068 has a normal atomic gas content for its SFR and is located close to most gas-poor galaxies within this relation. The relation has been established using over 1500 galaxies, also covering the SFR range relevant here.

We present the continuum map at an observed frequency of 1.397667 GHz in Fig. 3. We detected two point sources within

Table 1. H_I properties of CGCG 137-068.

Beam (")	z_{HI}	W_{50} (km s ⁻¹)	W_{10} (km s ⁻¹)	F_{int} (Jy km s ⁻¹)	$\log(L'_{\text{HI}})$ (K km s ⁻¹ pc ²)	$\log(M_{\text{HI}})$ (M_{\odot})
(1)	(2)	(3)	(4)	(5)	(6)	(7)
28	0.013972 ± 0.000014	50 ± 30	127 ± 9	0.94 ± 0.09	10.738 ± 0.038	8.909 ± 0.038
19	0.013976 ± 0.000014	48 ± 22	127 ± 18	1.02 ± 0.12	10.772 ± 0.048	8.944 ± 0.048
13	0.013983 ± 0.000017	47 ± 22	126 ± 26	1.17 ± 0.15	10.832 ± 0.051	9.004 ± 0.051
5	0.013988 ± 0.000022	33 ± 14	126 ± 34	1.49 ± 0.23	10.939 ± 0.063	9.111 ± 0.063

Notes. (1) Beam size of the H_I cube (the global estimates are the most reliable for the coarsest resolution). (2) Redshift determined from the emission-weighted frequency of the H_I line. (3) H_I line width at the 50% of the maximum. (4) Width at the 10% of the maximum. (5) Integrated flux within the dotted lines in Fig. 1. (6) H_I line luminosity using Eq. (3) in Solomon et al. (1997). (7) Neutral hydrogen mass using Eq. (2) in Devereux & Young (1990).

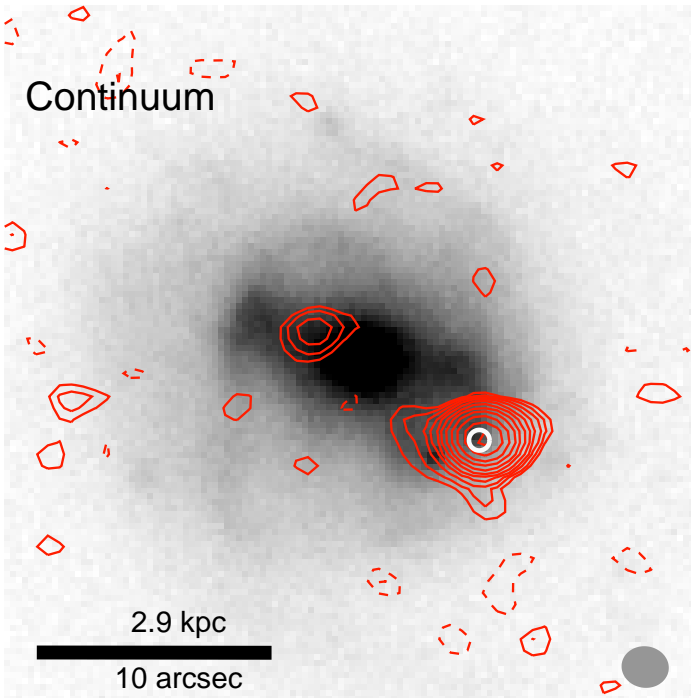


Fig. 3. Continuum GMRT 1.4 GHz contours (red) of CGCG 137-068 on the Gran Telescopio Canarias optical i' -band image of the galaxy (Kann et al., in prep.). The lowest contour is at 2σ ($\sigma = 17 \mu\text{Jy beam}^{-1}$) and the steps are in factors of $\sqrt{2}$. The VLBI position of AT 2018cow is indicated by the white circle. We detected the emission of AT 2018cow at this position and an additional object in the north-eastern part of the galaxy. The beam size of the radio data is shown as the grey circle. The image is $30'' \times 30''$ and the scale is indicated by the ruler. North is up and east is to the left.

CGCG 137-068: AT 2018cow in the south-west and a second source at the north-eastern part of the bar, just outside the bulge. The positions, fluxes, and SFRs using the conversion of Bell (2003) are listed in Table 2. For the first source we show the SFR as an upper limit, as it is dominated by AT 2018cow. This is motivated by a small offset ($0.24''$) of this source to the VLBI position of AT 2018cow and the fact that a variable 1.4 GHz flux at this level has been reported by Margutti et al. (2019).

The SFR of the second source ($0.081 M_{\odot} \text{ yr}^{-1}$) is $37_{-8}^{+7}\%$ of the total SFR of the galaxy as measured from the spectral energy distribution modelling ($0.22 M_{\odot} \text{ yr}^{-1}$; Perley et al. 2019). This source is coincident with one of the peaks of the H_I maps.

Table 2. Properties of the continuum 1.397667 GHz sources within CGCG 137-068.

RA (h m s)	Dec (d m s)	$F_{1.4\text{GHz}}$ (mJy)	$\text{SFR}_{\text{radio}}$ ($M_{\odot} \text{ yr}^{-1}$)
16 16 00.209	+22 16 04.78	1.239 ± 0.018	<0.565
16 16 00.729	+22 16 09.52	0.101 ± 0.018	0.081 ± 0.011

Notes. The first object corresponds to AT 2018cow. We treated its radio SFR estimate (using the conversion of Bell 2003) as an upper limit because AT 2018cow has a significant contribution to the radio flux. The mean time of the observations is 2019-02-08-17.41667 UT (237.28470 days after the optical discovery).

The analogous continuum source is not present in the other half of the bar on the other side of the bulge. Star formation along the bar and differences between the two halves of the bar are common among local spirals, but regions inside bars do not dominate the total SFR (Regan et al. 1996; Sheth et al. 2000, 2002; Koda & Sofue 2006; Momose et al. 2010; Hirota et al. 2014; Yajima et al. 2019). Moreover, barred spirals always exhibit significant star formation in the galaxy centre, which is not evident for CGCG 137-068.

The SFR and stellar mass of CGCG 137-068 (Perley et al. 2019) imply a specific SFR ($\text{sSFR} \equiv \text{SFR}/M_{*}$) of $\sim 0.15 \text{ Gyr}^{-1}$. At this stellar mass, the sSFR of a main-sequence galaxy is $\sim 0.2 \text{ Gyr}^{-1}$ (Speagle et al. 2014). Hence, CGCG 137-068 is a main-sequence galaxy at the bottom of the scatter of this relation with no enhancement or strong suppression of star formation.

The atomic gas and star formation properties of CGCG 137-068 are summarised in Fig. 4 and compared with GRB/SN hosts with H_I measurements (Michałowski et al. 2015, 2018a). For each galaxy we also show the predicted gas depletion time from the M_{HI} -SFR relation (Michałowski et al. 2015). GRB/SN hosts occupy two regions of this diagram: either on or below the main-sequence and abundant with atomic gas (high gas depletion timescale well above the prediction), or above the main-sequence with low gas depletion timescale, due to elevated SFR. In contrast, CGCG 137-068 is below the main sequence, but it has a lower gas content than predicted from the M_{HI} -SFR relation. In particular, it is different than the hosts of GRB 060505 and 111005A, which have 0.3–0.5 dex more atomic gas than predicted from their SFR. In terms of the M_{HI}/SFR ratio, the AT 2018cow host is most similar to the GRB 980425 host, which is, however, at the upper boundary of the main sequence and exhibits a strong gas concentration close to the GRB position, unlike the AT 2018cow host.

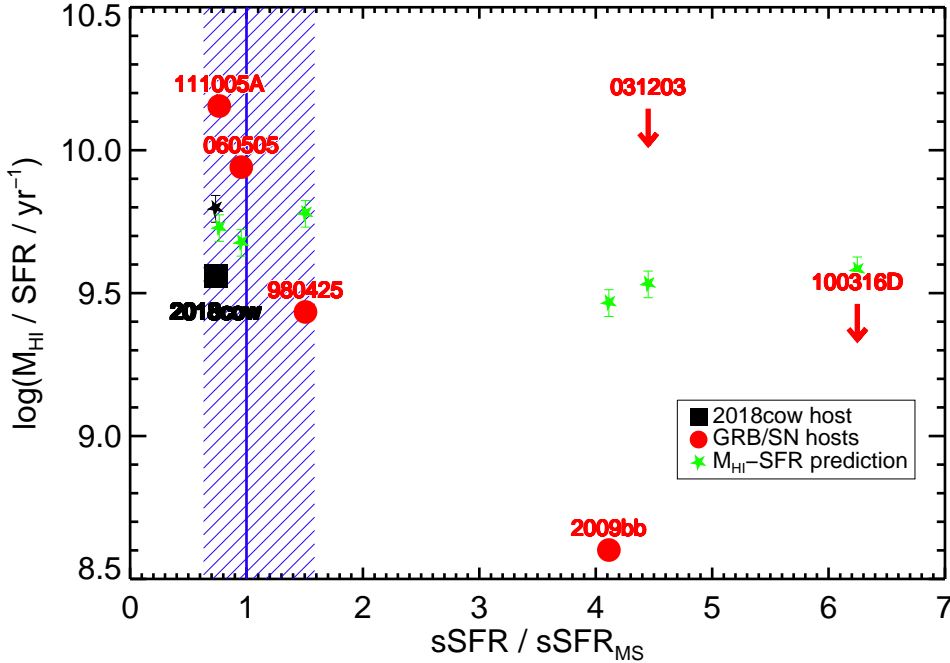


Fig. 4. Atomic gas depletion timescale ($\equiv M_{\text{HI}}/\text{SFR}$) as a function of the ratio of the sSFR to the main-sequence sSFR at a given redshift and stellar mass (Speagle et al. 2014). CGCG 137-068 and GRB/SN hosts (Michałowski et al. 2015, 2018a) are shown as a black square and red circles and arrows, respectively. The main sequence and its scatter are shown as a blue vertical solid line and the hatched region, respectively. For each galaxy, a black or green star shows the predicted gas depletion time for its SFR from the M_{HI} -SFR relation (Michałowski et al. 2015). The errors include both the uncertainty in the SFRs and in the parameters of the relation.

4. Discussion

The atomic gas distribution of CGCG 137-068 does not show strong unusual features (especially not at the position of AT 2018cow), in contrast to the off-centre gas concentrations and irregular velocity fields of the host galaxies of GRBs or relativistic SNe (Arabsalmani et al. 2015; Michałowski et al. 2014, 2015, 2016, 2018a). Moreover, there is no enhancement of the SFR, which could be a signature of a gas inflow. The environment of AT 2018cow therefore suggests that its progenitor may not have been a massive star (Prentice et al. 2018; Margutti et al. 2019; Rivera Sandoval et al. 2018; Fox & Smith 2019). However, the GRB/SN host sample with atomic gas measurements is small, so we cannot rule this hypothesis out.

The asymmetry in the distribution of atomic gas in the case of the host of the relativistic SN 2009bb may be a result of interaction (Michałowski et al. 2018a), as has also been observed for other galaxies (Sancisi et al. 2008; Rasmussen et al. 2006). To investigate this further, we therefore analysed the large-scale environment of CGCG 137-068 using the NASA/IPAC Extragalactic Database (NED) of CGCG 137-068. It seems fairly isolated, with no other galaxies within 500 kpc projected distance and 1000 km s⁻¹ velocity. The nearest galaxy is UGC 10322, more than 500 kpc away in projected distance. This means that no galaxy in the current catalogues is close enough to significantly influence the properties of CGCG 137-068. We found that CGCG 137-068 is ~700 kpc to the west of a possible galaxy group extending several hundred kiloparsec across and containing six galaxies. Similarly to the host of SN 2009bb (Michałowski et al. 2018a), this could mean that there is a supply of intergalactic gas available for inflow onto CGCG 137-068, but we did not find any evidence of this process.

On the other hand, all other proposed explosion mechanisms of AT 2018cow, except for massive-star core-collapse, should not result in a connection between its progenitor and gas concentration or inflow: an exploding low-mass hydrogen-rich star (Margutti et al. 2019), a TDE (Liu et al. 2018; Kuin et al. 2019; Perley et al. 2019), and a merger of white dwarfs or a neutron star and a giant star (Lyutikov & Toonen 2018; Soker et al. 2019).

The normal atomic gas distribution of CGCG 137-068 is therefore consistent with these mechanisms.

After the submission of this paper, the results of Roychowdhury et al. (2019) on the atomic gas distribution in the host galaxy of AT 2018cow were published. They found a ring of gas that is also visible in our combined dataset (Fig. 2).

As claimed by Roychowdhury et al. (2019), such a gas ring could be the result of a minor merger. However, most rings in galaxies have been shown to be the result of resonances caused by the presence of a bar (gravitational torques; see the review by Buta & Combes 1996) and other internal mechanisms, such as viscous torques (Icke 1979; Buta 1986; Lesch et al. 1990; Combes & Gerin 1985; Armillotta et al. 2019). Similarly, Díaz-García et al. (May 2019) found an increasing fraction of ringed galaxies with increasing bar Fourier density amplitude (also for galaxies with stellar masses similar to that of CGCG 137-068).

CGCG 137-068 indeed exhibits a strong bar that might be the cause of the appearance of the gas ring. Moreover, the H I velocity fields presented here and by Roychowdhury et al. (2019) do follow a rotation pattern, and do not show any sign of disturbances based on the errors in the measurements. Finally, almost all spiral galaxies (including those with similar masses to CGCG 137-068) exhibit central depressions of atomic gas (likely due to conversion to the molecular phase) or enhancement at the location of the spiral arms (Leroy et al. 2008; Bigiel & Blitz 2012; Martinsson et al. 2016). This feature, combined with low sensitivity (as in the highest resolution map of Roychowdhury et al. 2019) would give rise to a ring-like structure in the data, which would have a purely internal origin. The gas ring in CGCG 137-068 without any sign of disturbance is therefore not strong evidence of a recent merger.

5. Conclusions

We observed the H I atomic hydrogen line emission of the AT 2018cow host galaxy with the Giant Metrewave Radio Telescope. There is no unusual atomic gas concentration near the position of AT 2018cow. The gas distribution is much more regular than those of the hosts of GRBs and SNe. The atomic gas mass of the AT 2018cow host is lower by 0.24 dex than the prediction

from its SFR and is at the lower edge of the galaxy main sequence. In the continuum we detected the emission of AT 2018cow and of a star-forming region in the north-eastern part of the bar (away from AT 2018cow). This region hosts a third of the galaxy SFR.

The absence of atomic gas concentration close to AT 2018cow, along with a normal SFR and regular H α velocity field sets CGCG137-068 apart from GRB/SN hosts studied in H α . The environment of AT 2018cow therefore suggests that its progenitor may not have been a massive star. Our findings are consistent with an origin of the transient that does not require a connection between its progenitor and gas concentration or inflow: an exploding low-mass star, a tidal disruption event, or a merger of white dwarfs or of a neutron star and a giant star. We interpret the recently reported atomic gas ring in CGCG 137-068 as a result of internal processes connected with gravitational resonances caused by the bar.

Acknowledgements. We thank Joanna Baradziej for help in improving this paper. M.J.M. acknowledges the support of the National Science Centre, Poland, through the POLONEZ grant 2015/19/P/ST9/04010 and SONATA BIS grant 2018/30/E/ST9/00208; this project has received funding from the European Union's Horizon 2020 research and innovation programme under the Marie Skłodowska-Curie grant agreement No. 665778. P.K. is supported by the BMBF project 05A17PC2 for D-MeerKAT J.H. was supported by a VILLUM FONDEN Investigator grant (project number 16599). D.A.K. acknowledges support from the Juan de la Cierva Incorporación fellowship IJCI-2015-26153. A.d.U.P. and C.C.T. acknowledge support from Ramón y Cajal fellowships (RyC-2012-09975 and RyC-2012-09984). D.A.K., A.d.U.P., and C.C.T. acknowledge support from the Spanish research project AYA2017-89384-P. L.K.H. acknowledges funding from the INAF PRIN-SKA program 1.05.01.88.04. The Cosmic Dawn Center is funded by the DNRF. R.L. acknowledges support from the grant EMR/2016/007127 from the Dept. of Science and Technology, India. This project has received funding from the European Research Council (ERC) under the European Union's Horizon 2020 research and innovation programme (grant agreement no. 679627; project name FORNAX; PI Paolo Serra). We thank the staff of the GMRT who have made these observations possible. GMRT is run by the National Centre for Radio Astrophysics of the Tata Institute of Fundamental Research. Based on observations made with the Gran Telescopio Canarias (GTC), in the Roque de los Muchachos Observatory. We acknowledge the usage of the HyperLeda database (<http://leda.univ-lyon1.fr>). This research has made use of the NASA/IPAC Extragalactic Database (NED), which is operated by the Jet Propulsion Laboratory, California Institute of Technology, under contract with the National Aeronautics and Space Administration; SAOImage DS9, developed by Smithsonian Astrophysical Observatory (Joye & Mandel 2003); and NASA's Astrophysics Data System Bibliographic Services.

References

- An, T. 2018, *ATel.*, 12067
- Arabsalmani, M., Roychowdhury, S., Zwaan, M. A., Kanekar, N., & Michałowski, M. J. 2015, *MNRAS*, 454, L51
- Armillotta, L., Krumholz, M. R., Di Teodoro, E. M., & McClure-Griffiths, N. M. 2019, *MNRAS*, submitted [arXiv:1905.01309]
- Becker, R. H., White, R. L., & Helfand, D. J. 1995, *ApJ*, 450, 559
- Bell, E. F. 2003, *ApJ*, 586, 794
- Benetti, S., Pastorello, A., Cappellaro, E., et al. 2018, *ATel.*, 11836
- Bietenholz, M., Margutti, R., Alexander, K., et al. 2018, *ATel.*, 11900
- Bigiel, F., & Blitz, L. 2012, *ApJ*, 756, 183
- Bright, J., Horesh, A., Fender, R., et al. 2018, *ATel.*, 11774
- Buta, R. 1986, *ApJ*, 61, 609
- Buta, R., & Combes, F. 1996, *Fund. Cosmic Phys.*, 17, 95
- Chabrier, G. 2003, *ApJ*, 586, L133
- Combes, F. 2018, *A&ARv*, 26, 5
- Combes, F., & Gerin, M. 1985, *A&A*, 150, 327
- de Ugarte Postigo, A., Bremer, M., Kann, D. A., et al. 2018, *ATel.*, 11749
- Devereux, N. A., & Young, J. S. 1990, *ApJ*, 359, 42
- Díaz-García, S., Díaz-Suárez, S., Knäpen, J. H., & Salo, H. May 2019, *A&A*, 625, A146
- Dobie, D., Ravi, V., Ho, A., Kasliwal, M., & Murphy, T. 2018, *ATel.*, 11795
- Elmegreen, B. G., Herrera, C., Rubio, M., et al. 2018, *ApJ*, 859, L22
- Fox, O. D., & Smith, N. 2019, *MNRAS*, submitted [arXiv:1903.01535]
- Hatsukade, B., Ohta, K., Endo, A., et al. 2014, *Nature*, 510, 247
- Hirota, A., Kuno, N., Baba, J., et al. 2014, *PASJ*, 66, 46
- Ho, A. Y. Q., Phinney, E. S., Ravi, V., et al. 2019, *ApJ*, 871, 73
- Horesh, A., Moldon, J., Beswick, R., et al. 2018, *ATel.*, 11819
- Icke, V. 1979, *A&A*, 78, 21
- Iverson, R. J., Greve, T. R., Dunlop, J. S., et al. 2007, *MNRAS*, 380, 199
- Izzo, L., de Ugarte Postigo, A., Kann, D. A., et al. 2018, *ATel.*, 11753
- Joye, W. A., & Mandel, E. 2003, in *Astronomical Data Analysis Software and Systems XII*, eds. H. E. Payne, R. I. Jedrzejewski, & R. N. Hook, *ASP Conf. Ser.*, 295, 489
- Kenyon, J. S., Smirnov, O. M., Grobler, T. L., & Perkins, S. J. 2018, *MNRAS*, 478, 2399
- Koda, J., & Sofue, Y. 2006, *PASJ*, 58, 299
- Kuin, N. P. M., Wu, K., Oates, S., et al. 2019, *MNRAS*, 487, 2505
- Leroy, A. K., Walter, F., Brinks, E., et al. 2008, *AJ*, 136, 2782
- Lesch, H., Biermann, P. L., Crusius, A., et al. 1990, *MNRAS*, 242, 194
- Liu, L. D., Zhang, B., Wang, L. J., & Dai, Z. G. 2018, *ApJ*, 868, L24
- Lyutikov, M., & Toonen, S. 2018, ArXiv e-prints [arXiv:1812.07569]
- Makarov, D., Prugniel, P., Terekhova, N., Courtois, H., & Vauglin, I. 2014, *A&A*, 570, A13
- Margutti, R., Metzger, B. D., Chornock, R., et al. 2019, *ApJ*, 872, 18
- Martinson, T. P. K., Verheijen, M. A. W., Bershad, M. A., et al. 2016, *A&A*, 585, A99
- McMullin, J. P., Waters, B., Schiebel, D., Young, W., & Golap, K. 2007, in *Astronomical Data Analysis Software and Systems XVI*, eds. R. A. Shaw, F. Hill, & D. J. Bell, *ASP Conf. Ser.*, 376, 127
- Michałowski, M. J., Hunt, L. K., Palazzi, E., et al. 2014, *A&A*, 562, A70
- Michałowski, M. J., Gentile, G., Hjorth, J., et al. 2015, *A&A*, 582, A78
- Michałowski, M. J., Castro Cerón, J. M., Wardlow, J. L., et al. 2016, *A&A*, 595, A72
- Michałowski, M. J., Gentile, G., Krühler, T., et al. 2018a, *A&A*, 618, A104
- Michałowski, M. J., Karska, A., Rizzo, J. R., et al. 2018b, *A&A*, 617, A143
- Michałowski, M. J., Xu, D., Stevens, J., et al. 2018c, *A&A*, 616, A169
- Momose, R., Okumura, S. K., Koda, J., & Sawada, T. 2010, *ApJ*, 721, 383
- Narayanan, D., Turk, M., Feldmann, R., et al. 2015, *Nature*, 525, 496
- Nayana, A. J., & Chandra, P. 2018, *ATel.*, 11950
- Offringa, A. R. 2010, AOFlogger: RFI Software
- Offringa, A. R., McKinley, B., Hurley-Walker, N., et al. 2014, *MNRAS*, 444, 606
- Perley, D. A., Mazzali, P. A., Yan, L., et al. 2019, *MNRAS*, 484, 1031
- Prentice, S. J., Maguire, K., Smartt, S. J., et al. 2018, *ApJ*, 865, L3
- Rasmussen, J., Ponman, T. J., & Mulchaey, J. S. 2006, *MNRAS*, 370, 453
- Regan, M. W., Teuben, P. J., Vogel, S. N., & van der Hulst, T. 1996, *AJ*, 112, 2549
- Rivera Sandoval, L. E., Maccarone, T. J., Corsi, A., et al. 2018, *MNRAS*, 480, L146
- Roychowdhury, S., Arabsalmani, M., & Kanekar, N. 2019, *MNRAS*, 485, L93
- Sánchez, Almeida J., Elmegreen, B. G., Muñoz-Tuñón, C., & Elmegreen, D. M. 2014, *A&ARv*, 22, 71
- Sancisi, R., Fraternali, F., Oosterloo, T., & van der Hulst, T. 2008, *A&ARv*, 15, 189
- Schaye, J., Dalla, Vecchia C., Booth, C. M., et al. 2010, *MNRAS*, 402, 1536
- Serra, P., Westmeier, T., Giese, N., et al. 2015, *MNRAS*, 448, 1922
- Sheth, K., Regan, M. W., Vogel, S. N., & Teuben, P. J. 2000, *ApJ*, 532, 221
- Sheth, K., Vogel, S. N., Regan, M. W., et al. 2002, *AJ*, 124, 2581
- Smartt, S. J., Clark, P., Smith, K. W., et al. 2018, *ATel.*, 11727
- Smith, I. A., Tanvir, N. R., & Perley, D. A. 2018, *ATel.*, 11781
- Soker, N., Grichener, A., & Gilkis, A. 2019, *MNRAS*, 484, 4972
- Solomon, P. M., Downes, D., Radford, S. J. E., & Barrett, J. W. 1997, *ApJ*, 478, 144
- Speagle, J. S., Steinhardt, C. L., Capak, P. L., & Silverman, J. D. 2014, *ApJS*, 214, 15
- Spring, E. F., & Michałowski, M. J. 2017, *MNRAS*, 471, L101
- Stanway, E. R., Levan, A. J., Tanvir, N. R., Wiersema, K., & van der Laan, T. P. R. 2015, *ApJ*, 798, L7
- Thöne, C. C., Izzo, L., Flores, H., et al. 2019, *A&A*, submitted [arXiv:1904.05935]
- Tonry, J. L., Denneau, L., Heinze, A. N., et al. 2018, *PASP*, 130, 064505
- van de Voort, F., Schaye, J., Altay, G., & Theuns, T. 2012, *MNRAS*, 421, 2809
- White, R. L., Becker, R. H., Helfand, D. J., & Gregg, M. D. 1997, *ApJ*, 475, 479
- Willett, K. W., Lintott, C. J., Bamford, S. P., et al. 2013, *MNRAS*, 435, 2835
- Xu, D., Wang, J., Xin, L., et al. 2018, *ATel.*, 11740
- Yajima, Y., Sorai, K., Kuno, N., et al. 2019, *PASJ*, psz022

¹ Astronomical Observatory Institute, Faculty of Physics, Adam Mickiewicz University, ul. Słoneczna 36, 60-286 Poznań, Poland e-mail: mj.michalowski@gmail.com

² Astronomisches Institut der Ruhr-Universität Bochum (AIRUB), Universitätsstrasse 150, 44801 Bochum, Germany

- ³ DARK, Niels Bohr Institute, University of Copenhagen, Lyngbyvej 2, 2100 Copenhagen Ø, Denmark
- ⁴ Instituto de Astrofísica de Andalucía (IAA-CSIC), Glorieta de la Astronomía, s/n, 18008 Granada, Spain
- ⁵ PITT PACC, Department of Physics and Astronomy, University of Pittsburgh, Pittsburgh, PA 15260, USA
- ⁶ The Cosmic Dawn Center, Niels Bohr Institute, University of Copenhagen, Lyngbyvej 2, 2100 Copenhagen Ø, Denmark
- ⁷ ARIES, Manora Peak, Nainital 263002, India
- ⁸ INAF-Osservatorio Astrofisico di Arcetri, Largo E. Fermi 5, 50125 Firenze, Italy
- ⁹ Finnish Centre for Astronomy with ESO (FINCA), University of Turku, Väisäläntie 20, 21500 Piikkiö, Finland
- ¹⁰ Tuorla Observatory, Department of Physics and Astronomy, University of Turku, Väisäläntie 20, 21500 Piikkiö, Finland
- ¹¹ Laboratoire AIM-Paris-Saclay, CEA/DSM/Irfu – CNRS – Université Paris Diderot, CE-Saclay, pt courrier 131, 91191 Gif-sur-Yvette, France
- ¹² Department of Physics, University of California, 1 Shields Ave, Davis, CA 95616-5270, USA
- ¹³ Thüringer Landessternwarte Tautenburg, Sternwarte 5, 07778 Tautenburg, Germany
- ¹⁴ INAF-OAS Bologna, Via Gobetti 93/3, 40129 Bologna, Italy
- ¹⁵ Technical University of Denmark, Department of Physics, Fysikvej, building 309, 2800 Kgs. Lyngby, Denmark
- ¹⁶ Indian Institute of Space Science & Technology, Thiruvananthapuram 695547, India
- ¹⁷ Physics Department, University of Calabria, 87036 Arcavacata di Rende, Italy
- ¹⁸ Department of Physics, University of Bath, Bath BA2 7AY, UK
- ¹⁹ Department of Particle Physics and Astrophysics, Weizmann Institute of Science, Rehovot 7610001, Israel
- ²⁰ South African Radio Astronomy Observatory, 2 Fir Street, Black Rivetexr Park, Observatory, Cape Town, South Africa
- ²¹ Department of Physics and Electronics, Rhodes University, PO Box 94, Grahamstown 6140, South Africa
- ²² Argelander-Institut für Astronomie, Auf dem Hügel 71, 53121 Bonn, Germany
- ²³ INAF – Osservatorio Astronomico di Cagliari, Via della Scienza 5, 09047 Selargius, CA, Italy